Characterization of Ethylene-1-Hexene Copolymers Made with Supported Metallocene Catalysts: Influence of Support Type

Beatriz Paredes,[1] *João B.P. Soares,**[2] *Rafael van Grieken,*[1] *Alicia Carrero,*[1] *Inmaculada Suarez*[1]

Summary: It is known that the nature of the support, as well as the technique used to anchor the metallocene onto it, play important roles on catalytic activity and on the properties of the polymers produced with supported metallocenes. In the present work, the effect of different support types on the microstructure of ethylene/1-hexene copolymers made with supported metallocene catalysts has been investigated through the analysis of molecular weight and chemical composition distributions using high temperature gel permeation chromatography (GPC) and crystallization analysis fractionation (Crystaf). The copolymer samples obtained using commercial carriers (silica and silica-alumina) had unimodal chemical composition distributions and were used to create a linear calibration curve relating the peak crystallization temperature from Crystaf and the comonomer content as determined by ^{13}C NMR. This calibration curve is useful to determine the 1-hexene fractions for each peak in the resins showing bimodal chemical composition distributions, such as those obtained with catalysts supported on MCM-41 and SBA-15 materials. The structure and chemistry of the support used had a large influence on comonomer incorporation and the shape of the chemical composition distribution of the polymer, which suggests that the supporting process creates different types of active sites.

Keywords: crystallization analysis fractionation (Crystaf); MCM-41; SBA-15; silica-alumina; supported metallocene catalysts

Introduction

Metallocene catalysis can be considered a major breakthrough in polyolefin production technology. The discovery of metallocene/alkylaluminoxane systems allowed the synthesis of polyolefins with very different properties from those made with Ziegler-Natta catalysts.

Metallocenes combine high activity with excellent polymer microstructural control[1] but, because they are homogeneous catalysts, they produce polymer particles with ill-defined morphologies that cause reactor fouling when used in slurry reactors. On the other hand, these catalysts have been used very effectively in solution processes by several companies worldwide.

The immobilization of metallocenes on supports is a technical and economical solution to these limitations.[2] Moreover, to replace the conventional heterogeneous Ziegler–Natta catalysts used in industrial slurry and gas-phase processes with metallocene catalysts (drop-in technology), metallocene catalysts have to be immobilized on supports. It is important to find a way to attach the metallocene to the support without losing the performance of the homogeneous complex, while improving the morphology of the polymer particles.[3]

[1] Department of Chemical and Environmental Technology, ESCET, Universidad Rey Juan Carlos, 28933 Mostoles, Spain
[2] Department of Chemical Engineering, University of Waterloo, Waterloo, Ontario N2L 3G1, Canada
E-mail: jsoares@cape.uwaterloo.ca

In general, when a metallocene catalyst is supported, its activity decreases because of the significant steric hindrance around the active site caused by the large support surface, deactivation of catalytic sites, or inefficient production of active sites during the supporting process.[4] It is known that the nature of the support, as well as the technique used to anchor the metallocene onto it, play important roles on catalytic activity and on the properties of the polymers produced with supported metallocenes.[5]

There are three basic methods of supporting aluminoxane-activated single-site catalysts: (1) supporting the aluminoxane first, then reacting the aluminoxane-treated support with the metallocene; (2) supporting the metallocene first, then reacting the metallocene-treated support with the aluminoxane; and (3) contacting the aluminoxane and the metallocene in solution before supporting and then adding this solution to the support. The last method has some advantages over the other two: It maximizes the number of active centers by activating the metallocene in solution instead of carrying out the process with either the metallocene or the aluminoxane immobilized on the support, reduces the preparation time, and lowers the amount of solvent required for supporting.[6]

There are many publications describing the heterogeneization of metallocenes onto supports such as silica,[7–10] alumina,[11] magnesium chloride,[12] starch,[13] zeolites,[14] cyclodextrin,[15] and synthetic polymers.[16,17] Metallocenes can also be attached onto the inner surface of mesoporous molecular sieves.[18] The large surface areas of mesoporous molecular sieves can provide high dispersion of the metallocenes. These materials allow studying the effect of different structural variables, such as pore size, pore volume and surface areas, and of chemical properties by varying the ratio of silicon to aluminium during support synthesis.[19] These properties may have a significant influence on the catalytic behaviour of metallocenes and on the properties of the obtained polymer.

In this work, mesostructured MCM-41 materials[20] with different Si/Al ratio and SBA-15 materials[21] with different pore sizes have been used to immobilize $(nBuCp)_2ZrCl_2$/MAO. Commercial carriers such as silica and silica-alumina have also been investigated for comparison.

Metallocene catalysts are generally believed to have uniform site types even after being supported. In general, polymers produced by supported metallocenes have narrow molecular weight distributions (MWD)[22,23] with polydispersity indexes close to two or slightly higher. Some supported metallocenes may also make polyolefins with broad MWDs, which has been associated with the formation of several active site types[24] and/or mass transfer resistances during polymerization.

The effect of different support types has been studied for the copolymerization of ethylene and 1-hexene. For the case of copolymers, besides MWD determination, it is necessary to measure the chemical composition distribution (CCD) to have a more complete understanding of active site types and polymer properties. Therefore, in this study the influence of support type has been investigated through the analysis of MWD and CCD using high temperature gel permeation chromatography (GPC) and crystallization analysis fractionation (Crystaf), respectively. It will be shown that polyolefins having a narrow MWD can have a very broad and multimodal CCD, indicating the presence of more than one active site type during the polymerization.

Experimental Part

Synthesis of the Carriers and Preparation of Supported Catalysts

Commercial carriers silica and silica-alumina from W.R. Grace were heat-treated at 400 °C and at 200 °C, respectively, for 5 hours before use.

The MCM-41 supports were synthesized in basic medium at room temperature[20] using hexadecyltrimethylammonium bromide (C_{16}TABr, 99 wt%, Aldrich) as

surfactant, water, dimethylamine (DMA, 40 wt%, Aldrich), tetraethyl ortosilicate (TEOS, 98 wt%, Aldrich) as the silica source, and aluminium (molar ratio of Si/Al = 15, 60 and infinite) was incorporated during synthesis using aluminium isopropoxide (AIP, 99 wt%, Aldrich) as the aluminium source. The surfactant was first dissolved in water and DMA. The mixture of TEOS and AIP was added to this solution to form the MCM-41 supports. The final mixture was subjected to an ageing procedure at 105 °C for 48 hours. Finally, the resulting material was filtered and calcined at 550 °C for 5 hours in static conditions.

The SBA-15 supports were prepared according to a direct synthesis procedure previously published in the literature[21,25–27] in acidic medium at 40 °C using pluronic $EO_{20}PO_7EO_{20}$ (P123, Aldrich) as surfactant, hydrochloric acid (HCl, 35 wt%, Sharlau) and tetraethyl ortosilicate (TEOS, 98 wt%, Aldrich) as the silica source. The surfactant was first dissolved in a solution of HCl (pH = 1.5), then TEOS was added and the mixture was kept at 40 °C for 20 h. In order to make silica SBA-15 supports with different pore sizes 1,3,5-trimethylbenzene (TMB, 98 %wt, Aldrich) and n-decane (98 wt%, Fluka) were used as swelling agents. After crystallization, they were aged at 105 °C for 24 hours. Finally, the resulting material was filtered and calcined at 500 °C for 5 hours under dry air flow.

Heterogeneous catalysts were prepared by impregnating commercial and synthesized supports with a mixture ($Al_{(MAO)}$/Zr = 170 mol/mol) of methylaluminoxane (MAO 30 wt% in toluene, Witco) and a solution of bis(butylcyclopentadienyl) zirconium dichloride ($(nBuCp)_2ZrCl_2$, Crompton) in dry toluene (99 wt%, Scharlab) under inert nitrogen atmosphere using Schlenk techniques and a glove box. The ratio between the volume of impregnating solution and support pore volume was three. The reaction was performed at room temperature, in a stirred vessel during 3 hours. The supported catalyst was dried under nitrogen flow and stored in a glove-box.

Characterization of Supports and Catalysts

Nitrogen adsorption-desorption isotherms at 77 K were obtained with a Micromeritics Tristar 2050 apparatus. The samples were previously out-gassed under vacuum at 200 °C for 2 hours. Surface areas were calculated by means of the BET equation whereas mean pore size was obtained from the maximum of BJH pore size distribution.

Polymerization and Polymer Characterization

Polymerizations were performed at 70 °C in a 1 litter stirred-glass reactor. The ethylene flow rate was followed by a mass-flow indicator in order to keep the reactor pressure at 5 bar during the polymerization. Different amounts of 1-hexene were injected into the reactor with a syringe at the beginning of the polymerization. In these reactions, tri-isobutylamunimum (TIBA, 30 wt% in heptane, Witco) was added as scavenger in an $Al_{(TIBA)}$/Zr molar ratio of 400. After 30 minutes, the polymerization was stopped by depressurization and quenched by addition of acidified (HCl) methanol. The polymer obtained was separated by filtration and dried under atmospheric pressure at 70 °C.

Molecular weight averages and distributions were determined with a Waters ALLIANCE GPCV 2000 gel permeation chromatograph (GPC) equipped with a refractometer, a viscosimeter and three Styragel HT type columns (HT3, HT4 and HT6) with exclusion limit 1×10^7 for polystyrene. 1,2,4-Trichlorobenzene was used as solvent, at a flow rate of 1 cm^3min^{-1}. The analyses were performed at 145 °C. The columns were calibrated with standard narrow molar mass distribution polystyrenes and with linear low density polyethylenes and polypropylenes.

Polymer melting points (T_m), crystallization temperatures (T_c) and crystallinities were determined in a METTLER TOLEDO DSC822 differential scanning calorimeter (DSC), using a heating rate of 10 °Cmin^{-1} in the temperature range 23–160 °C. The heating cycle was performed twice, but only the results of the second

Table 1.
Physical properties of the supports.

Support	SiO_2	SiO_2-Al_2O_3	MCM-41 Si/Al			SBA-15 swelling agent		
			15	60	infinite	none	n-decane	TMB
Average pore diameter (nm)[a)]	28.5	18.2	2.1	2.4	2.5	8.8	11.3	22.7
BET surface area (m^2/g)	285	370	837	1015	1129	628	608	588
Pore volume (cm^3/g)	1.55	1.29	0.58	0.77	0.77	1.16	0.78	1.73

[a)] Determined from the maximum of BJH pore size distribution.

scan are reported, because the former is influenced by the mechanical and thermal history of the samples.

Chemical composition distributions were measured by Crystaf (Polymer Char) using 1,2,4-trichlorobenzene as a solvent. Dissolution took place at 160 °C for 90 min followed by equilibration at 95 °C for 45 min. The crystallization rates were 0.1 °C/min from 95 to 19 °C. A two channel infrared detector was used to measure the concentration of polymer in the solution during crystallization.

A BRUKER AC300 spectrometer at 75 MHz was used to characterize the copolymers by ^{13}C NMR measurement and determine their 1-hexene molar fraction. The samples were added into sample tube (a diameter of 5 mm) with the mixture of 1,2,4-trichlorobenzene and 1,1,2,2-tetrachloroethylane-d_2 in a concentration of 10 vol%. Each sample was measured with 10 s pulse repetition.

Results and Discussion

The main physical properties of the commercial and synthesized materials are summarized in Table 1. The nitrogen adsorption–desorption isotherms at 77 K (not shown) belonged to type IV of the I.U.P.A.C classification corresponding to mesoporous materials. As it can been observed in the table, three MCM-41 materials with similar pore diameter and different silicon to aluminium molar ratio were obtained, and three SBA-15 carriers with different pore size, as a function of the swelling agent employed in the synthesis, were prepared. The effect of the structure and chemical properties of support material on the ethylene-1-hexene copolymerization has been investigated using these materials as supports of the catalytic system $(nBuCp)_2ZrCl_2$/MAO.

All the supported catalysts had good activities for polymerization, with activities varying from 0.46 to $9.91 \cdot 10^6$ g PE/mol $Zr \cdot h \cdot bar$, observing a positive comonomer effect with a different maximum value depending on the support employed.

Molecular weight averages of polymers made with $(nBuCp)_2ZrCl_2$/MAO supported on the commercial carriers were not affected significantly when 1-hexene was added (Table 2). The polydispersity index

Table 2.
Characterization of poly(ethylene-*co*-1-hexene) samples made with $(nBuCp)_2ZrCl_2$/MAO supported on commercial carriers.

Support	mL 1-hexene	0	5	15	25	35	50	60	75
SiO_2	$\overline{M}_n$(g/mol)	81061	53853	55415	58336	64847	67197	73903	75450
	$\overline{M}_w/\overline{M}_n$	2.91	3.06	2.76	2.58	2.59	2.58	2.79	2.91
	T_m (°C)	133	122	113	108	104	95	94	91
	T_c (°C)	116	112	98	98	91	86	86	73
	Crystallinity (%)	64	51	40	37	22	27	25	19
SiO_2-Al_2O_3	$\overline{M}_n$ (g/mol)	70613	48307	44687	47541	78729	67887	77617	52250
	$\overline{M}_w/\overline{M}_n$	2.89	2.70	2.63	2.78	2.62	2.87	3.09	3.28
	T_m (°C)	132	122	115	109	104	96	104	94
	T_c (°C)	117	111	102	95	87	78	85	79
	Crystallinity (%)	64	51	43	36	30	24	28	24

($\overline{M}_w/\overline{M}_n$) varied from 2.58 to 3.28, higher than the value of 2.0 expected for homogeneous single-site catalysts, suggesting some heterogeneity in the nature of the active sites.[28] Melting and crystallization temperatures decreased with increasing comonomer content, as expected.

Figure 1 shows the Crystaf profiles of the polymers produced with $(nBuCp)_2ZrCl_2$/MAO supported on SiO_2 and SiO_2-Al_2O_3. Crystallization temperatures are correlated to the comonomer content.[29] As all of them have narrow, unimodal CCDs, they are useful to create a calibration curve since it covers a broad range of comonomer incorporation.[30] The linear relationship between Crystaf peak temperature, T_{peak}, and the molar fraction of 1-hexene measured by ^{13}C NMR is illustrated in Figure 2.

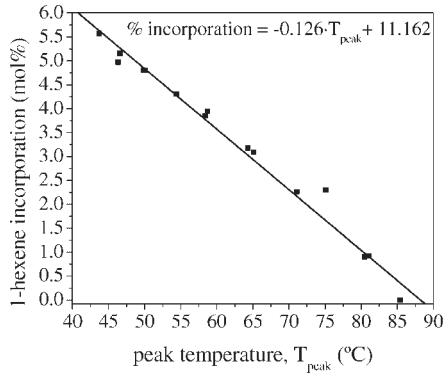

Figure 2.
Crystaf calibration curve for poly(ethylene-*co*-1-hexene) made with $(nBuCp)_2ZrCl_2$/MAO supported on commercial carriers.

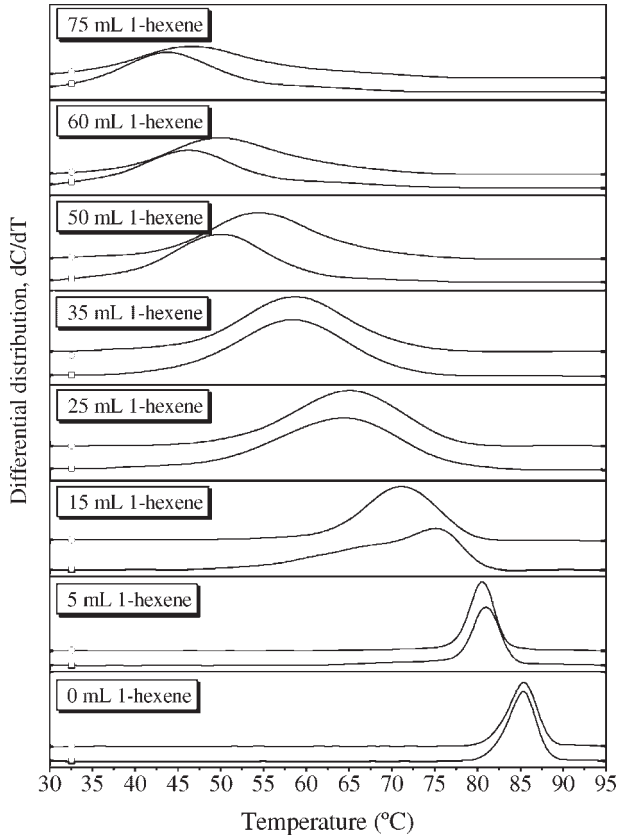

Figure 1.
Crystaf profiles of poly(ethylene-*co*-1-hexene) made with $(nBuCp)_2ZrCl_2$/MAO supported on commercial carriers: □ SiO_2 and ○ SiO_2-Al_2O_3.

Several investigations have pointed out that the formation and stabilization of zirconium cations (Zr^+) may be easier when support materials have surface acidic properties.[3,31] In this work, we have studied this phenomenon through the use of synthesized MCM-41 materials with different silicon to aluminium molar ratios. Table 3 shows that the acidity of the support does not have a significant influence on the properties of the copolymers, apart from those related with the incorporation of higher amounts of the α-olefin. When MCM-41 is used, the MWD continues to be narrow, but the CCD broadens significantly with increasing 1-hexene content and even becomes bimodal for certain 1-hexene concentrations, as shown in Figure 3. This may be related to the presence of two catalyst site types on the surface of the support. Therefore, the Si/Al ratio can be used to control the shape of the CCD. Interestingly, lower temperature peaks become more prominent with decreasing Si/Al ratios.

Another important property affecting the behaviour of support materials for metallocenes is pore size, since the support has to be able to anchor the catalyst precursor, the cocatalyst, and permit easy access to the active sites for the monomers.[18] The geometrical constraints of the parallel hexagonal channel structure of the SBA-15 materials may affect the pattern of monomer insertion and chain growth process, which offers a way to control the polymer chain structure and morphology during the polymerization.[32] To study this effect, we have synthesized three SBA-15 materials with different pore sizes using several swelling agents, as described above.

Table 4 summarizes the properties of the poly(ethylene-*co*-1-hexene) made with $(nBuCp)_2ZrCl_2$/MAO supported on SBA-15 materials. The MWD is still narrow, but the CCD can also become broad and bimodal, as depicted in Figure 4. Larger pore sizes seem to favour 1-hexene incorporation slightly, which may be related in part to intraparticle mass transfer resistances.

Finally, we have calculated the overall mol% of 1-hexene for the copolymer samples obtained with $(nBuCp)_2ZrCl_2$/MAO supported on both MCM-41 and SBA-15 using the calibration curve shown in Figure 2. These results are reported in Table 5, together with overall 1-hexene mol% measured with ^{13}C NMR. The good agreement between the two techniques indicates that our calibration curve also works well for the bimodal CCD copolymers made with $(nBuCp)_2ZrCl_2$/MAO supported on both MCM-41 and SBA-15.

Table 3.
Characterization of the poly(ethylene-*co*-1-hexene) made with $(nBuCp)_2ZrCl_2$/MAO immobilized on supports synthesized with different Si/Al ratios.

Support	mL 1-hexene	0	5	25	50	75
MCM-41-15	$\overline{M}_n$ (g/mol)	62358	37521	44796	63216	54288
	$\overline{M}_w/\overline{M}_n$	2.95	2.85	2.94	3.3	3.58
	T_m (°C)	136	124	109	103	100
	T_c (°C)	113	110	95	95	82
	Crystallinity (%)	66	54	36	32	26
MCM-41-60	$\overline{M}_n$(g/mol)	60915	38927	46271	60234	52746
	$\overline{M}_w/\overline{M}_n$	2.9	2.7	2.75	3.09	3.85
	T_m (°C)	133	123	110	110	110
	T_c (°C)	116	110	91	94	86
	Crystallinity (%)	62	53	36	32	31
MCM-41-infinite	$\overline{M}_n$(g/mol)	67674	40961	46713	40065	51420
	$\overline{M}_w/\overline{M}_n$	3.21	3.07	3.07	4.25	4
	T_m (°C)	133	124	110	111	108
	T_c (°C)	116	110	91	93	102
	Crystallinity (%)	65	52	37	34	32

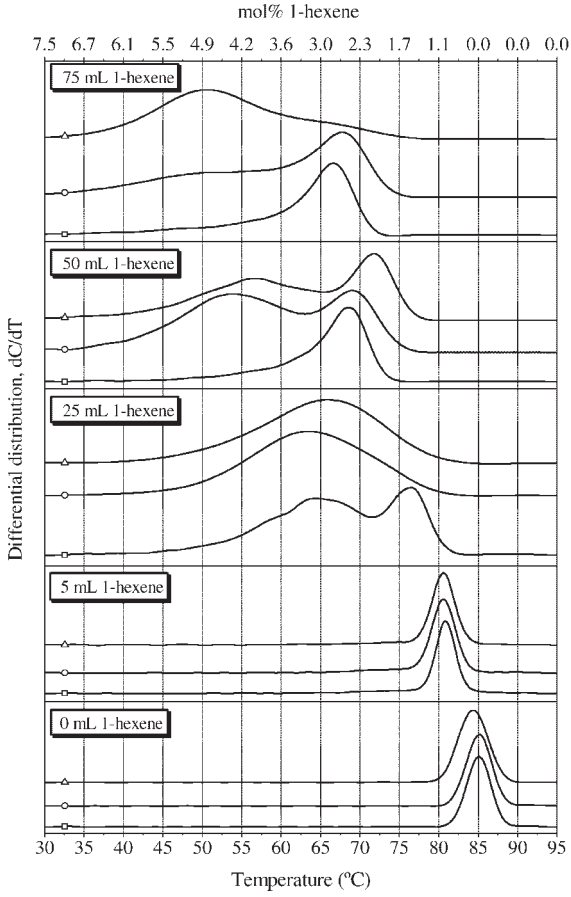

Figure 3.
Crystaf profiles of poly(ethylene-*co*-1-hexene) made with $(nBuCp)_2ZrCl_2$/MAO supported on MCM-41 with different Si/Al molar ratios: □ infinite; ○ 60 and △ 15. The mol% 1-hexene upper *x*-axis was calculated using the calibration curve in Figure 2.

Table 4.
Characterization of the poly(ethylene-*co*-1-hexene) made with $(nBuCp)_2ZrCl_2$/MAO immobilized on supports synthesized with different pore sizes.

Support	mL 1-hexene	0	5	25	50	75
SBA-15	$\overline{M}_n$ (g/mol)	74530	48869	55640	49333	68525
	$\overline{M}_w/\overline{M}_n$	2.67	2.47	2.67	3.01	3.22
	T_m (°C)	133	124	113	113	108
	T_c (°C)	116	111	95	93	88
	Crystallinity (%)	65	53	38	31	30
SBA-15-n-decane	$\overline{M}_n$ (g/mol)	53530	34968	43432	55751	58114
	$\overline{M}_w/\overline{M}_n$	2.78	2.66	2.69	3.03	3.44
	T_m (°C)	133	122	112	108	108
	T_c (°C)	117	109	94	89	91
	Crystallinity (%)	66	52	37	34	28
SBA-15-TMB	$\overline{M}_n$ (g/mol)	61391	44489	48885	59091	87092
	$\overline{M}_w/\overline{M}_n$	2.67	2.61	2.60	2.80	2.93
	T_m (°C)	133	123	110	106	102
	T_c (°C)	116	112	95	85	82
	Crystallinity (%)	65	50	37	29	26

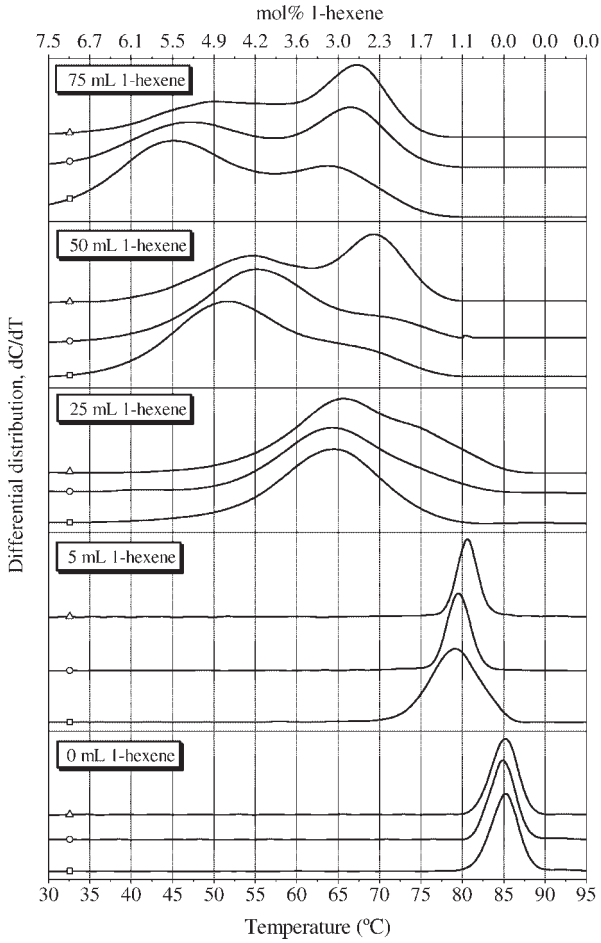

Figure 4.
Crystaf profiles of poly(ethylene-*co*-1-hexene) made with $(nBuCp)_2ZrCl_2$/MAO supported on SBA-15 with different pore sizes: □ 22.7 nm; ○ 11.3 nm and △ 8.8 nm. The mol% 1-hexene upper *x*-axis was calculated using the calibration curve in Figure 2.

Conclusions

All the poly(ethylene-*co*-1-hexene) samples made with $(nBuCp)_2ZrCl_2$/MAO supported on SiO_2, SiO_2/Al_2O_3, MCM-41 with different Si/Al ratios, or SBA-15 with different pore size, had narrow MWD, but CCDs that could vary from narrow and unimodal to broad and bimodal. The CCDs of copolymers made with $(nBuCp)_2ZrCl_2$/MAO supported on SiO_2 and SiO_2/Al_2O_3 were always unimodal, but those made with MCM-41 and SBA-15 became bimodal with increasing 1-hexene content. This bimodality may be related to the presence of two catalyst site types on the surface of the support. Lower Crystaf temperature peaks (that is, polymer populations with higher 1-hexene fractions) became more prominent with decreasing Si/Al ratio, and larger pore sizes seemed to favour 1-hexene incorporation slightly.

This investigation demonstrates that copolymer samples that do not differ significantly in their MWD shapes can have totally distinct CCD profiles as measured by Crystaf. Therefore, Crystaf (or equivalently, temperature rising elution fractionation,

Table 5.
Comparison of 1-hexene mol% of poly(ethylene-*co*-1-hexene) samples measured by ^{13}C NMR and calculated with the Crystaf calibration curve.

Support	mol% 1- hexene ^{13}C NMR	mol% 1- hexene calibration curve
MCM-41-15	0.79	1.05
	3.12	3.08
	3.54	3.77
	4.39	4.49
MCM-41-60	0.94	1.09
	3.10	3.17
	3.74	3.79
	3.75	3.71
MCM-41-infinite	0.80	1.04
	2.83	2.67
	2.90	2.91
	3.35	3.26
SBA-15	0.76	1.00
	2.67	2.68
	3.44	3.42
	3.72	3.72
SBA-15- n-decane	0.87	1.16
	2.87	2.95
	4.20	3.89
	4.22	4.11
SBA-15-TMB	0.79	1.21
	3.01	3.18
	4.32	4.24
	4.71	4.71

TREF) is an essential analysis to characterize copolymers made with coordination catalysts, even when they are expected to behave as single-site type catalysts.

[1] J. H. Z. dos Santos, A. Larentis, M. Barbosa da Rosa, C. Krug, I. J. R. Baumbol, J. Dupont, F. C. Stedile, M. D. C. Forte, *Macrom. Chem. Phys.* **1999**, *200*(4), 751.
[2] G. Fink, R. Mülhaupt, H. H. Brintzinger, Ziegler Catalyst: Recent Innovations and Technological Improvements, Springer-Verlag, Berlin **1995**, 42.
[3] M. R. Ribeiro, A. Deffieux, M. F. Portela, *Ind. Eng. Chem. Res.* **1997**, *36*(4), 1224.
[4] K.-J. Chu, J. B. P. Soares, A. Penlidis, *J. Polym. Sci., Part A: Polym. Chem.* **2000**, *38*, 462.
[5] A. E. Hamielec, J. B. P. Soares, *Prog. Polym. Sci.* **1996**, *21*, 651.
[6] G. G. Hlatky, *Chem. Rev.* **2000**, *100*(4), 1347.
[7] Eur. Patent 336,593, M. Chang.
[8] U.S. Patent 4,912,075, M. Chang.
[9] K. Soga, M. Kaminaka, *Makromol. Chem. Rapid Commun.* **1992**, *13*, 221.
[10] J. C. W. Chien, D. He, *J. Polym. Sci., Part A: Polym. Chem.* **1991**, *29*, 1603.
[11] S. K. Ihm, K. J. Chu, J. H. Yim, In Catalyst Design for Tailor-Made Polyolefins, K. Soga, M. Terano, Eds., Elsevier-Kodansa, Tokyo **1994**, 299.
[12] M. Kaminaka, K. Soga, *Makromol. Chem. Rapid Commun.* **1991**, *12*, 367.
[13] U.S. Patent 4,431,788, W. Kaminsky.
[14] Y. S. Ko, T. K. Han, J. W. Park, S. I. Woo, *Macromol. Rapid Commun.* **1996**, *17*, 749.
[15] D. Y. Lee, K. B. Yoon, *Macromol. Rapid Commun.* **1994**, *15*, 841.
[16] U.S. Patent 4,921,825, M. Kioka, N. Kashiwa.
[17] U.S. Patent 5,362,824, A. B. Furtek, R. S. Shinomoto.
[18] D. Trong On, D. Desplantier-Giscard, C. Danumah, S. Kaliaguine, *Appl. Catal. A-Gen.* **2001**, *222*(1–2), 299.
[19] U. Ciesla, F. Schuth, *Micropor. Mesopor. Mat.* **1999**, *27*, 131.
[20] W. Lin, Q. Cai, W. Pang, Y. Yue, B. Zou, *Micropor. Mesopor. Mat.* **1999**, *33*, 187.
[21] D. Zhao, J. Feng, Q. Huo, N. Melosh, H. Fredrickson, B. Chmelka, G. D. Stucky, *Science* **1998**, *279*, 548.
[22] S. Jüngling, S. Koltzenburg, R. Mülhaupt, *J. Polym. Sci., Part A: Polym. Chem.* **1997**, *35*, 1.
[23] K. Soga, M. Kaminaka, *Makromol. Chem.* **1993**, *194*, 1745.
[24] J. D. Kim, J. B. P. Soares, G. L. Rempel, *J. Polym. Sci., Part A: Polym. Chem.* **1999**, *37*, 331.
[25] Y. Wang, M. Noguchi, Y. Takahashi, Y. Ohtsuka, *Catal. Today* **2001**, *68*, 3.
[26] E. Byambajav, Y. Ohtsuka, *Appl. Catal. A-Gen* **2003**, *252*(1), 193.
[27] Y.-H. Yue, A. Gedeon, J.-L. Bonardet, J. B. d'Espinose, N. Melosh, J. Fraissard, in: A. Sayari, M. Jaroniec, T. J. Pinnavaia, Eds., *Stud. Surf. Sci. Catal.* **2000**, *129*, 209.
[28] D. Bianchini, K. M. Bichinho, J. H. Z. dos Santos, *Polymer* **2002**, *43*(10), 2937.
[29] B. Monrabal, J. Blanco, J. Nieto, J. B. P. Soares, *J. Polym. Sci., Part A: Polym. Chem.* **1999**, *37*, 89.
[30] D. M. Sarzotti, J. B. P. Soares, A. Penlidis, *J. Polym. Sci., Part B: Polym. Phys.* **2002**, *40*, 2595.
[31] V. I. Costa, P. G. Belelli, J. H. Z. dos Santos, M. L. Ferreira, D. E. Damián, *J. Catal.* **2001**, *204*, 1.
[32] Z. Ye, H. Alsyouri, S. Zhu, Y. S. Lin, *Polymer* **2003**, *44*, 969.

